

Lawrence Berkeley National Laboratory

Recent Work

Title

EFFECT OF PROCESSING ON MICROSTRUCTURE AND MECHANICAL BEHAVIOR OF
MAGNESIUM OXIDE

Permalink

<https://escholarship.org/uc/item/2618f66s>

Authors

Sweeting, Truett B.
Pask, Joseph A.

Publication Date

1975-02-01

Submitted to Journal of the American
Ceramic Society

RECEIVED
LAWRENCE
RADIATION LABORATORY

LBL-3700
Preprint c. |

MAR 14 1975

LIBRARY AND
DOCUMENTS SECTION

EFFECT OF PROCESSING ON MICROSTRUCTURE AND
MECHANICAL BEHAVIOR OF MAGNESIUM OXIDE

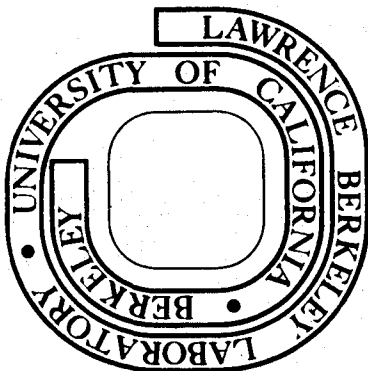
Truett B. Sweeting and Joseph A. Pask

February 1975

Prepared for the U. S. Atomic Energy Commission
under Contract W-7405-ENG-48

For Reference

Not to be taken from this room



LBL-3700
c. |

DISCLAIMER

This document was prepared as an account of work sponsored by the United States Government. While this document is believed to contain correct information, neither the United States Government nor any agency thereof, nor the Regents of the University of California, nor any of their employees, makes any warranty, express or implied, or assumes any legal responsibility for the accuracy, completeness, or usefulness of any information, apparatus, product, or process disclosed, or represents that its use would not infringe privately owned rights. Reference herein to any specific commercial product, process, or service by its trade name, trademark, manufacturer, or otherwise, does not necessarily constitute or imply its endorsement, recommendation, or favoring by the United States Government or any agency thereof, or the Regents of the University of California. The views and opinions of authors expressed herein do not necessarily state or reflect those of the United States Government or any agency thereof or the Regents of the University of California.

EFFECT OF PROCESSING ON MICROSTRUCTURE
AND MECHANICAL BEHAVIOR OF MAGNESIUM OXIDE

Truett B. Sweeting* and Joseph A. Pask

Inorganic Materials Research Division, Lawrence Berkeley Laboratory
and Department of Materials Science and Engineering,
College of Engineering; University of California,
Berkeley, California 94720

ABSTRACT

Specimens of polycrystalline MgO were fabricated from two powders after varying preparation procedures by hot pressing in graphite or alumina dies, followed by annealing in air, vacuum, or within the graphite die in vacuum. Impurities introduced and modified throughout the entire processing procedure resulted in microstructures with varying grain size and grain boundary structure. The formation of a liquid phase in one type tended to eliminate the effect of these processing variables but led to the development of larger grain sizes. Correlations of the microstructures of the specimens were made with their mechanical behavior in compression at a constant strain rate at 1200°C.

*Based on a thesis submitted by T. B. Sweeting for the M.S. degree in ceramic engineering.

I. INTRODUCTION

Dense, fine grained polycrystalline MgO has been fabricated by hot pressing. Spriggs et al.¹ produced nearly theoretically dense MgO at 1120°C and 13,000 psi. Leipold and Nielson² obtained theoretically dense specimens at 800°C and 10,000 psi, which on subsequent heating in air showed rapid grain growth and no reheat porosity. The influence of water vapor on the hot pressing of MgO was studied by Shelly and Nicholson.³ Presence of impurity anions was found to retard densification; bloating and clouding were also observed, which were attributed to pressure building up from the entrapped gases.⁴⁻⁷

Mechanical behavior at elevated temperatures is dependent on microstructural features of the specimens. The importance of the nature of the grain boundary has been shown in experiments conducted in tension,⁸ bending,⁹ and compression.^{10,11} Most recently, Snowden and Pask¹² attributed differences of behavior of specimens fabricated by several procedures utilizing hot pressing as a step to resulting differences in grain boundary structure.

In this study, the first objective was to contribute to the understanding of the role of processing conditions in hot pressing on microstructure development, and then to determine the relation between mechanical behavior and microstructural features with particular emphasis placed on the nature of the grain boundary.

II. EXPERIMENTAL PROCEDURE

(1) Characterization of MgO Powders

Two magnesia powders were used in this study, and will hereafter be referred to as Type I and Type II. The major difference in their

analyses (Table 1) was the higher Si, Ca and sulfate contents in Type II.

Differential thermal analysis (DTA) and thermogravimetric analysis (TGA) were obtained in air at a heating rate of 10°C/min up to 1000°C. An endothermic reaction was shown beginning about 265°C and peaking at 360°C for both types of MgO which is in good agreement with the results of Chown and Deacon¹³ for hydrated magnesia; the intensity, however, was higher for Type I. The weight losses occurred within the same temperature range but more gradually for Type II which also was still losing weight at 1000°C. This was probably due to the higher sulfate content of Type II since MgSO₄ has a decomposition pressure of 1 atm at 1125°C.

Table I also contains physical data on the MgO powders. The surface area was measured by adsorption from an iodine solution. The reactivity was measured by mixing two grams of powder with citric acid and noting the time to endpoint using phenolphthalein as an indicator, a shorter time being indicative of great reactivity. Powder of Type II was twice as reactive and had five times the surface area as that of Type I.

X-ray diffraction patterns for both powders did not indicate the presence of any second phase. The crystallite size was determined by a method outlined by Rau¹⁴ using the Scherrer equation.

(2) Powder Preparation

Preliminary specimens prepared from an unmilled powder were found to contain undesirable microstructural inhomogeneities which were attributed to agglomeration in the starting powder. This led to an investigation into the following powder processing procedures, using Type I powder that had been first screened to remove the coarsest aggregates, to evaluate their effectiveness in reducing such defects:

- (1) Dry milled 2h -- alumina balls.
- (2) Dispersion in isopropanol, dried, dry milled 2h -- alumina balls.
- (3) Dry milled 2h -- teflon balls.
- (4) Wet milled 1h, dried, dry milled 2h -- teflon balls.

The ball milling was done in a 2-liter, rubber lined mill, using 55 grams of powder in each case. The dispersion step in (2) consisted of gradual addition of the 55 grams of unmilled powder to 275 ml of isopropanol, while stirring "magnetically." The resulting mixture was placed in an ultrasonic cleaner for two minutes to aid dispersion. The suspension was then dried 24 h at 90°C, resulting in a "cakelike" structure which was broken up manually before ball milling. In (4) the powder was dispersed as in (2), but an additional 250 ml of isopropanol was added during dispersion; this mixture was wet milled one h before drying within the mill for 24 h at 90°C. This treatment was followed by the dry milling step. The powders were then hot pressed in graphite dies and annealed in air.

(3) Specimen Preparation for Mechanical Testing

Disks, 2 in. dia., were prepared from both powders by using the selected powder preparation procedure and then hot pressing them in graphite and alumina dies. With the graphite die, a thin (.005") graphite foil sleeve was used along the die cavity wall. Graphite foil spacers were also used between the powder and the plunger faces. The powder was cold pressed at 2000 psi outside of the furnace, so that measurements could be taken to determine green density. The die was placed in the hot press, and evacuated to 10^{-4} Torr before heating. The

heating cycle consisted of heating at 8°C/min to 1250°C with arrests at 500°C for 15 min and 1000°C for one h to allow gas from decompositions to escape, and finally at 1250°C for 30 min. Pressure of 3000 psi was applied at 1200°C and maintained constant through the hold at 1250°C. Pressure was then released and the specimen was furnace-cooled. A similar procedure was followed for the alumina die; however, a heating rate of 5°C/min was used to minimize thermal gradients across the die wall. Molybdenum spacers were used to separate the powder from the plunger faces to prevent sticking and reaction. Because of the low density of the Type I MgO specimen produced by this procedure, a specimen was made applying pressure at 1100°C and gradually increasing it to a maximum of 6500 psi at 1200°C. The pressure was then held constant to 1250°C and held 20 min. All of the disks were cut into specimens approximately .6 in. x .25 in. x .25 in., using a diamond blade.

Hot-pressing characteristics in the graphite die are shown in Fig. 1 by a plot of density obtained from the measurements of ram travel on hot pressing versus temperature. Some densification, greater for Type II powder, occurred between 800 and 1000°C. Type I then showed little change in density until pressure was applied at 1200°C, and densification continued until near the end of the 30 min hold period at 1250°C. Type II, on the other hand, started to further densify with increase of temperature after 1000°C and reached its final density only a few minutes after pressure was applied at 1200°C.

The specimens from the disk formed in the graphite die were annealed at 1550°C for two h in air, vacuum, and vacuum within the graphite die. A specimen was also annealed in air for 24 h in a quench furnace with

MoSi₂ elements. The vacuum anneal was done in a Brew furnace with tantalum heating elements. The annealing in the graphite die was done in vacuum in the hot press. Specimens from the disk formed in the alumina die received identical heat treatments, but were not annealed in the graphite die.

Approximately .15 in. was cut from the end of each test specimen. The internal surface of the end piece was used for microscopic examination. The polishing sequence consisted of using a series of emery papers through grade 4/0, followed by 6 μ m diamond paste with kerosene as a lubricant on a nylon cloth, and finally with 1 μ m diamonds on a Syntron vibrator. All samples were etched using .5M AlCl₃ at 50°C for about one min. Grain size determinations were made by counting the number of grains in a known area, converting to equivalent spherical diameter, and multiplying by a statistical factor of 1.28 or $4/\pi$.¹⁵ Over 500 grains were counted in each case.

Density measurements were made using a displacement technique in mercury. A value of 3.58 was taken as theoretical density of MgO to compute relative densities.

(4) Mechanical Testing

Specimens prepared for mechanical testing had a final length to width ratio of 2:1 and were approximately .36 in. x .18 in. x .18 in. The specimens were polished to these dimensions on a series of emery papers using a jig designed to keep faces parallel, and the ends flat, parallel, and perpendicular to the loading axis. Following this preparation, the specimens were chemically polished in 85% orthophosphoric acid at 110°C for two min.

All stress-strain data were obtained in compression at 1200°C at a constant strain rate of .025/min based on original sample height, using an Instron testing machine. The specimen was heated in a MoSi₂ element furnace at about 10°C/min, with a stabilization period of approximately 20 min at 1200°C before the start of the compression test. Platinum foil spacers prevented reaction between the specimen and the Lucalox Al₂O₃ buttoms used between the specimen and the loading rams. All stresses reported are based on original cross-sectional area, and all strains are true strains calculated from the recorded engineering strain. The amount of plastic strain was taken as the difference between the strain at .2% offset yield stress and the strain at the maximum stress recorded. The tests were run until the load started decreasing at an accelerating rate.

III. RESULTS AND DISCUSSION

(1) Microstructure Development

(A) Effect of Powder Preparation on Microstructure: Specimens prepared from unmilled Type I MgO powder by hot pressing in a graphite die and subsequent annealing in air had non-homogeneous microstructures as indicated by the presence of non-uniform regions of higher porosity and smaller grain size. Specimens were then formed from powders prepared by the four different procedures described previously. Density and grain size data are summarized in Table II.

The appearance of specimens after hot pressing varied: procedure (1), light gray and slightly translucent core covering approximately four-fifths of the cross-sectional area with the areas adjacent to the surfaces white; (2), similar but slightly lighter gray core; (3) and

unmilled powder, uniform white cross-sections; (4), very dark gray throughout. All specimens were white after annealing in air.

After hot pressing, the cores developed in (1) and (2) were attributed to contamination by organics introduced from the abrasion of the rubber-lined mill by the Al_2O_3 balls. In (3) and (4), the powder was contaminated by teflon on its surfaces during milling since MgO is harder than teflon. In addition, the dark gray color of (4) was attributed to contamination by organics from the rubber introduced by solution of the rubber by the isopropanol during the wet milling stage. The gray colors in (1), (2) and (4) were the result of some type of reaction involving rubber contamination and the carbonaceous atmosphere present in the graphite die during hot pressing. The white color of (3) indicates the absence of a dark carbonaceous residue on annealing teflon-contaminated specimens.

For all of the procedures, milling improved the homogeneity and increased the green density of the specimens. The rubber contamination did not significantly affect the densification process since the hot-pressed and annealed densities of (1) and (2) were essentially the same as the specimen prepared from the unmilled powder. The teflon contamination, on the other hand, significantly reduced the hot-pressed and annealed densities of (3) and (4) as seen in Table II. The Merck Index¹⁶ reports that teflon reverts to the gaseous monomer at 400°C; this must have been chemically adsorbed on the surfaces of the particles without forming a carbon residue.

Grain growth during annealing was significant in that the grain size for all of the hot-pressed specimens was only about 3 μm . After

annealing, the grain size was about the same for (1) and (2) as for the unmilled powder specimen, $\sim 30 \mu\text{m}$. The grain size for the specimens made from powders exposed to teflon, (3) and (4), was smaller, $\sim 20 \mu\text{m}$.

After analysis of the microstructures on the basis of homogeneity, density, and grain size, procedure (2), consisting of dispersion in isopropanol followed by dry milling with alumina balls, was chosen as the best procedure for the processing of both MgO powders for the fabrication of specimens for mechanical testing.

(2) Characterization of Test Specimens

(A) Type I MgO: In preparing specimens for mechanical testing, additional variables of hot pressing die (graphite or alumina) and ambient atmosphere during annealing (air, vacuum, or graphite die vacuum) were introduced. Also, specimens were made in the alumina die at two pressures. Table III summarizes data on density and grain size obtained on the Type I MgO specimens.

The specimen formed in the graphite die had a grayish core as described previously, whereas both specimens formed in the alumina die were white. The absence of any carbonaceous vapor species in the alumina die modified the reactions involving the contaminations introduced during preparation of the powder.

Samples from the specimen formed in the alumina die remained white upon annealing in air and vacuum. The higher density specimen which had pressure applied at a lower temperature showed a clouding of the center region after annealing in air, probably due to the formation of pores from entrapped gases, similar to that observed by Rice.¹⁷ The air anneal removed the grayish core from the samples hot pressed in the graphite

die, with little evidence of clouding. This difference in clouding was most likely attributable to the chemical nature of the residue along grain boundaries resulting from the difference in ambient atmospheres during hot pressing. The vacuum annealed specimen formed in the graphite die retained a faint gray core of about the same proportions but the core lost its slight translucency; the specimen annealed in the die was gray throughout.

The average grain size in the graphite die specimens annealed in different ambient atmospheres at 1550°C for 2 h was essentially constant ($\sim 29 \mu\text{m}$). Annealing in air for 24 h increased the grain size to about 60 μm . The number and size of pores varied although they were predominantly on grain boundaries.

The annealed specimens from the alumina die have considerably greater grain sizes, $\sim 40 \mu\text{m}$. This difference suggests that the ambient atmosphere during hot pressing has a significant effect on the nature of the grain boundary impurity and structure which subsequently affects grain growth during annealing. Thus, it was noted that the grain sizes for the annealed specimens from the alumina die were larger than that for the annealed specimens from unmilled powder hot pressed in the graphite die. These observations are in general agreement with reported results of MgO grain growth retardation by a fine dispersion of carbon.¹⁸

(B) Type II MgO: Table III also contains density and grain size for Type II MgO specimens fabricated in both dies and then annealed in various ambient atmospheres.

The disk hot pressed in the graphite die was gray and translucent throughout its entire cross section; in the alumina die, it was white

and translucent. Both samples were white after annealing in air but showed considerable clouding in their centers. In comparison with Type I MgO a significant decrease in density occurred on annealing, and white planar spots up to 3 mm in diameter developed just under the surface. Microscopic examination of the spots showed them to be voids between a denser outer layer and the cloudy porous center. It is believed that they were formed because the higher density of the outer region prevented the escape of gases generated in the interior. Similar spots were seen in the vacuum annealed specimens from both dies, but the spots were smaller and fewer in number. The graphite die annealed specimen was gray throughout and free of spots.

The clouding in the center on annealing in air can be attributed to the more rapid densification of Type II MgO specimens during hot pressing, and to the presence of sulfate. The overall undetermined reactions, however, are complex as indicated by a varying degree of cloudiness and spot formation on annealing in different ambient atmospheres.

Porosity was present mainly within the grains for all cases, and there was evidence of a second phase film along grain boundaries. This phase was attributed to the relatively high CaO and SiO₂ content of the Type II powder which led to the formation of a calcium-magnesium-silicate liquid phase during annealing at 1550°C. Leipold¹⁹ found segregation of Al, Si and Ca at grain boundaries during hot pressing even when present in average amounts as low as 30 ppm. This liquid phase presumably was responsible for the large increase in grain size by a solution-precipitation mechanism during annealing in comparison with the Type I MgO specimens, grain sizes of ~90 μm vs ~29 μm. Initial grain growth rates

are also fast, as indicated by a grain size of 74 μm with no holding time at 1550°C compared with 84 μm after an annealing time of 2 h.

The presence of the liquid phase also has apparently eliminated most of the atmospheric effects introduced during hot pressing since the grain size was similar for all annealed specimens of Type II MgO. For Type I MgO specimens the grain size was larger for the specimens formed by hot pressing in the alumina die.

(2) Mechanical Behavior

Stress-strain curves for the various annealed specimens formed in the graphite die, and the curves for the air annealed specimens formed in the alumina die, are shown in Fig. 2. The yield stress, maximum stress and plastic strain at maximum stress are summarized in Table III.

Macroscopic examination of the specimens after testing revealed that all Type I specimens contained visible vertical cracks near the center on one or more faces, whereas Type II specimens had cracks at the edges extending along the vertical length of the specimen as shown schematically in Fig. 3. In compression testing frictional forces develop between the specimen and the ram faces; these constraining forces lead to a barreling type of deformation which results in tensile stresses perpendicular to the loading direction and regions of high strain on the faces. Type II specimens, which showed little ductility, could not accommodate this high strain on the edges and fractured as illustrated. In contrast, Type I specimens, which exhibited much more ductility, accommodated the strain at the edges by yielding in shear and eventually began to fail in the center, the region of maximum tensile stress.

According to the Von Mises criteria for plasticity, plastic deformation by dislocation glide in polycrystalline MgO requires movement on five independent slip systems.²⁰ At 1200°C, dislocations can move first in favorably oriented grains on three (110) $\langle 1\bar{1}0 \rangle$ slip systems for which the yield stress for a conjugate pair is about 3000 psi at a stress rate of 20 psi/sec.²¹ Adjacent grains, however, may not be suitably oriented to allow the dislocations to move through the boundary, resulting in dislocation pile-ups that lead to stress concentrations. If the specimen has boundaries relatively free of impurities and porosity strong enough to maintain integrity to higher stress levels, slip may be initiated on three secondary (100) $\langle 1\bar{1}0 \rangle$ systems, for which the yield stress is about 18,000 psi at 1200°C with a stress rate of 20 psi/sec.²¹ Thus the five slip systems necessary for plastic deformation are activated. If the stress concentrations cannot be relieved by flow in adjacent grains, cracks may be nucleated at the grain boundary; and if the grain boundaries would be weak or impure, cracks may form at grain boundaries before plastic flow is realized in adjacent grains. The propagation of grain boundary cracks, however, is dependent on the nature of the grain boundaries.

Examining the mechanical behavior of the Type I specimens from the graphite die with 2 h anneals (Table III), the data show the yield stresses were similar yet the plastic strain was quite different; the air annealed specimen showed nearly three times as much strain as the die annealed specimen. Since the microstructure, including grain size and the amount and distribution of pores, was similar in each case, the significant variable must have been the nature of the grain boundary

after annealing. The character of the grain boundary of the air annealed specimen would be expected to be relatively free of carbonaceous impurities and more perfect in comparison with the die annealed specimen which was gray. The grain boundary structure of the latter does not transmit glide deformation as readily to adjoining grains as indicated by the smaller amount of plastic strain at the maximum stress. The vacuum annealed specimen would be expected to be intermediate in properties and behavior. The high yield stresses for these specimens in comparison with those for the slip systems of single crystals suggest the presence of grain boundaries in all cases that offer some resistance to nucleation and transmission of slip. There is, however, also the possibility that the higher strain rates in this study could have contributed to the higher yield stresses.

In the air annealed graphite die Type I MgO specimen, which presumably had the strongest grain boundaries, initial dislocation movement resulted in some plastic deformation. However, cracks began to develop between the most unfavorably oriented grains. These cracks did not readily propagate because of accommodation by some localized plastic deformation and lateral grain boundary separation akin to crack branching. The die annealed specimen, on the other hand, could not accommodate the initial cracks as easily because of less perfect grain boundaries. Therefore, once cracks were initiated their continued propagation was more probable, eventually leading to complete failure. SEM examination of fracture surfaces formed by breaking deformed specimens at room temperature, shown in Figs. 4 and 5, support this analysis. The fractured surface of the air annealed specimens show considerable cracking

and boundary separation; the die annealed specimen shows little separation and fewer cracks.

The Type I air annealed specimen from the alumina die showed reduced plasticity and yield stress in comparison with the air annealed specimen formed in the graphite die (Fig. 2). The grain size, however, is about 33% larger, 44 μm compared to 28 μm . A specimen from the graphite die annealed in air for 24 h showed even lesser plasticity, lower yield stress, and a larger grain size, 60 μm . Vasilos et al.²² reported a decrease in strength with increase of grain size, and Evans et al.⁹ showed a decrease in stress to initiate cracks by grain boundary dislocation pile-up with increasing grain size. Thus, increasing grain size for specimens similarly prepared increases the probability of forming a crack that will propagate to failure more readily.

The behavior of the Type II MgO specimens was markedly different from that of Type I but similar to each other (Fig. 2). This relationship was attributed to two factors: the presence of the second phase, and the large grain size. The presence of the second phase was verified by the debris on the fracture surfaces created at room temperature after the test, as seen in Figs. 6 and 7.

The brittle second phase along grain boundaries hinders dislocation nucleation and motion across grain boundaries due to stress concentrations developed by dislocation motion on easy slip systems generated within a single grain.²³ The resulting high stress concentrations were accommodated by the formation of cracks, which can be large in a large grain material. These long cracks led to failure at much lower stress levels and strains than those for the Type I MgO specimens. The brittle

second phase was the dominating factor and not the grain size as indicated by the fact that stress values for corresponding conditions were approximately four times larger for Type I than Type II MgO with a difference of only about 14 μm in grain size between the largest of Type I and smallest of Type II. Another significant effect of the second phase was to minimize the differences in grain boundary character introduced by variations in processing shown to exist for specimens made from Type I MgO.

IV. SUMMARY AND CONCLUSIONS

The role of impurities in determining the character of polycrystalline MgO specimens was seen to be significant throughout the entire processing procedure. The impurities associated with the starting MgO powder were significant in two ways: the anions OH^- , $\text{SO}_4^{=}$ and $\text{CO}_3^{=}$ played a role in the production of gases during hot pressing and annealing, and the cations Ca and Si led to the formation of a liquid phase during the annealing step which was distributed along grain boundaries and significantly increased the grain growth rate. The impurities introduced during the preparation of the powder were also significant. Contamination by rubber and teflon retarded grain growth on subsequent annealing. Grain boundary character was also affected by whether hot pressing was done in a graphite or alumina die and by the nature of the ambient atmosphere during annealing.

Specimens for mechanical behavior studies were fabricated from two MgO powders prepared by dispersing in isopropanol, drying, and milling in a rubber-lined mill with alumina balls. Specimens were then hot pressed in graphite and alumina dies, followed by annealing in air,

vacuum, and within the graphite die in vacuum. Type I MgO powder specimens had microstructures of varying grain size and grain boundary structure. Type II MgO powder specimens had a small amount of second phase along grain boundaries and essentially constant but larger grains. Stress-strain data was obtained in compression at a constant strain rate at 1200°C.

For specimens of Type I, the amount of plastic strain was determined by the nature of the grain boundary: the more perfect the boundary, the more strain at failure. In specimens with stronger and purer boundaries cracks could be essentially accommodated by localized plastic deformation at the crack tip, leading to progressive grain boundary separation akin to crack branching. The specimens with more imperfect grain boundaries could not accommodate cracks as easily, resulting in failure at lower maximum stresses and less strain at maximum stress.

For specimens of Type II MgO, grain boundary modifications and grain size variations during specimen preparation were minimized by the presence of a second phase. This phase led to failure at considerably lower stresses and strains.

The role of impurities introduced either in the powder or during processing in determining the grain boundary character and, in turn, the mechanical behavior was found to be critical. Grain boundary differences were interpreted in terms of differences in appearance and mechanical behavior. Further work is needed to determine the actual reactions taking place during the fabrication processes, and to characterize the grain boundary, in order to improve understanding of the grain boundary character-mechanical property relationship.

ACKNOWLEDGMENTS

Helpful discussions with William S. Snowden are gratefully acknowledged. Thanks are extended to Leonard Lee of Merck and Co. and Robert B. Langston of this laboratory for assistance in providing analytical data on the MgO powders.

This work was partially supported by the U. S. Energy Research and Development Administration and partially with the aid of a research grant from Kaiser Refractories Division of the Kaiser Aluminum and Chemical Co.

REFERENCES

1. R. Spriggs, L. Brisette, M. Rosett, and T. Vasilos, "Hot Pressing of Ceramics in Alumina Dies," Am. Ceram. Soc. Bull., 42 (9) 477-479 (1963).
2. M. Leipold and T. Nielsen, "Hot Pressing of High Purity MgO," Am. Ceram. Soc. Bull., 45 (3) 281-285 (1966).
3. R. Shelley and P. Nicholson, "Influence of Water Vapor on the Hot Pressing Kinetics of MgO," J. Am. Ceram. Soc., 54 (8) 365-367 (1971).
4. M. Leipold and C. Kapadia, "Effect of Anions of Hot Pressing of MgO," J. Am. Ceram. Soc., 56 (4) 200-203 (1973).
5. R. Rice, "Effect of Gaseous Impurities on the Hot Pressing and Behavior of MgO, Ca., and Al₂O₃," Proc. Brit. Ceram. Soc., 12 99 (1969).
6. T. Nielsen and M. Leipold, "Thermal Expansion in Air of Ceramic Oxides to 2200°C," J. Am. Ceram. Soc., 46 (8) 381-387 (1963).
7. R. Day and R. Stokes, "Grain Boundaries and the Mechanical Behavior of Magnesium Oxide," in Material Science Research, Vol. 3 edited by W. Kriegel and H. Palmour, III, Plenum Press, New York, 1966.
8. R. Day and R. Stokes, "Mechanical Behavior of Polycrystalline Magnesium Oxide at High Temperatures," J. Am. Ceram. Soc., 47 (10) 493-503 (1964).
9. A. Evans, D. Gilling, R. Davide, "The Temperature-Dependence of the Strength of Polycrystalline MgO," J. Mat. Sci., 5 187-197 (1970).
10. S. M. Copley and J. A. Pask, "Deformation of Polycrystalline MgO at Elevated Temperatures," J. Am. Ceram. Soc., 48 (12) 636-642 (1965).

11. T. G. Langdon and J. A. Pask, "Effect of Microstructure on Deformation of Polycrystalline MgO," J. Am. Ceram. Soc., 54 (5) 240-246 (1971).
12. W. E. Snowden and J. A. Pask, "High-Temperature Deformation of Polycrystalline Magnesium Oxide," Phil. Mag., 29 441-455 (1974).
13. J. Chown and R. Deacon, "The Hydration of Magnesia by Water Vapor," Trans. Brit. Ceram. Soc., 63 (2) 91-102 (1964).
14. R. Rau, "Measurement of Crystallite Size by Means of X-ray Diffraction Line-Broadening," Norelco Rep. X (3) 114-118 (1963).
15. R. L. Fullman, "Measurement of Particle Sizes in Opaque Bodies," Trans. A.I.M.E., 197 447-452 (1953).
16. Merck Index, 8th Edition, Ed. by P. Stecher, Merck & Co., Rahway, New Jersey, Copyright 1968.
17. R. Rice, "Production of Transparent MgO at Moderate Temperatures and Pressure," presented at 64th Annual Meeting of the Am. Ceram. Soc., New York, N.Y., April 30, 1962, Whitewares Div. No. 5-N-62.
18. A. C. Sugarman and J. R. Blachere, "Control of Grain Growth in MgO by a Fine Dispersion of Carbon," J. Am. Ceram. Soc., 57 (9) 414 (1974).
19. M. Leipold, "Impurity Distribution in MgO," J. Am. Ceram. Soc., 49 (9) 498-502 (1966).
20. R. von Mises, "Mechanics of Plastic Deformation of Crystals," Z. Agnew. Math. Mech., 8, 161 (1928).
21. C. O. Hulse, S. M. Copley and J. A. Pask, "Effect of Crystal Orientation of the Plastic Deformation of Magnesium Oxide," J. Am. Ceram. Soc., 46 (7) 317-323 (1963).

22. T. Vasilos, J. Mitchell and R. Spriggs, "Mechanical Properties of Pure, Dense Magnesium Oxide as a Function of Temperature and Grain Size," J. Am. Ceram. Soc., 47 (12) 601-610 (1964).
23. W. E. Snowden and J. A. Pask, "Microstructural Analysis and Stress-Strain Behavior of a Model Refractory System MgO-CaMgSiO₄," submitted to J. Am. Ceram. Soc.

Table I. Characterization of MgO powders

	Type I	Type II
<u>Chemical</u>		
†Al ₂ O ₃	.13%	.04%
††CaO	.21	.46
†FeO	.09	.06
†Na ₂ O	.014	.007
††SiO ₂	.06	.31
*Cl ⁻	.005	.021
*SO ₄ ⁼	.01	.22
*CO ₂	.71	.82
*H ₂ O	2.64	2.48
*Free moisture	0.37	0.28
*Loss on ignition	3.74	3.82
*MgCO ₃ , calculated	1.35	1.57
*Mg(OH) ₂ , calculated	8.6	8.8
<u>Physical</u>		
**Surface area, M ² /g	11.5	56.5
**Reactivity, sec.	87	44
X-ray crystallite size, Å	360	120

†Based on spectrographic analysis of elements, Lawrence Berkeley Lab., Univ. of Calif., Berkeley, Calif.

*Based on chemical analysis, Merck and Co., South San Francisco, Calif.

††Based on chemical analysis, Robert B. Langston, Inorganic Materials Research Div., Univ. of Calif., Berkeley, Calif.

**Performed by Merck and Co., South San Francisco, Calif.

Table II. Densities and grain sizes of Type I MgO Specimens produced by different processing procedures

Procedure	Green Density	Hot Pressed Density	Air Annealed Density	Average Grain Size
Unmilled	34	98.0	97.8	32
(1) Dry milled - alumina balls	39	98.0	97.8	30
(2) Dispersed, dry milled - alumina balls	46	98.5	98.2	28
(3) Dry milled - teflon balls	39	96.5	96.2	21
(4) Wet milled, dry milled - Teflon balls	41	95.5	95.1	19

Table III. Data for Type I and Type II MgO specimens

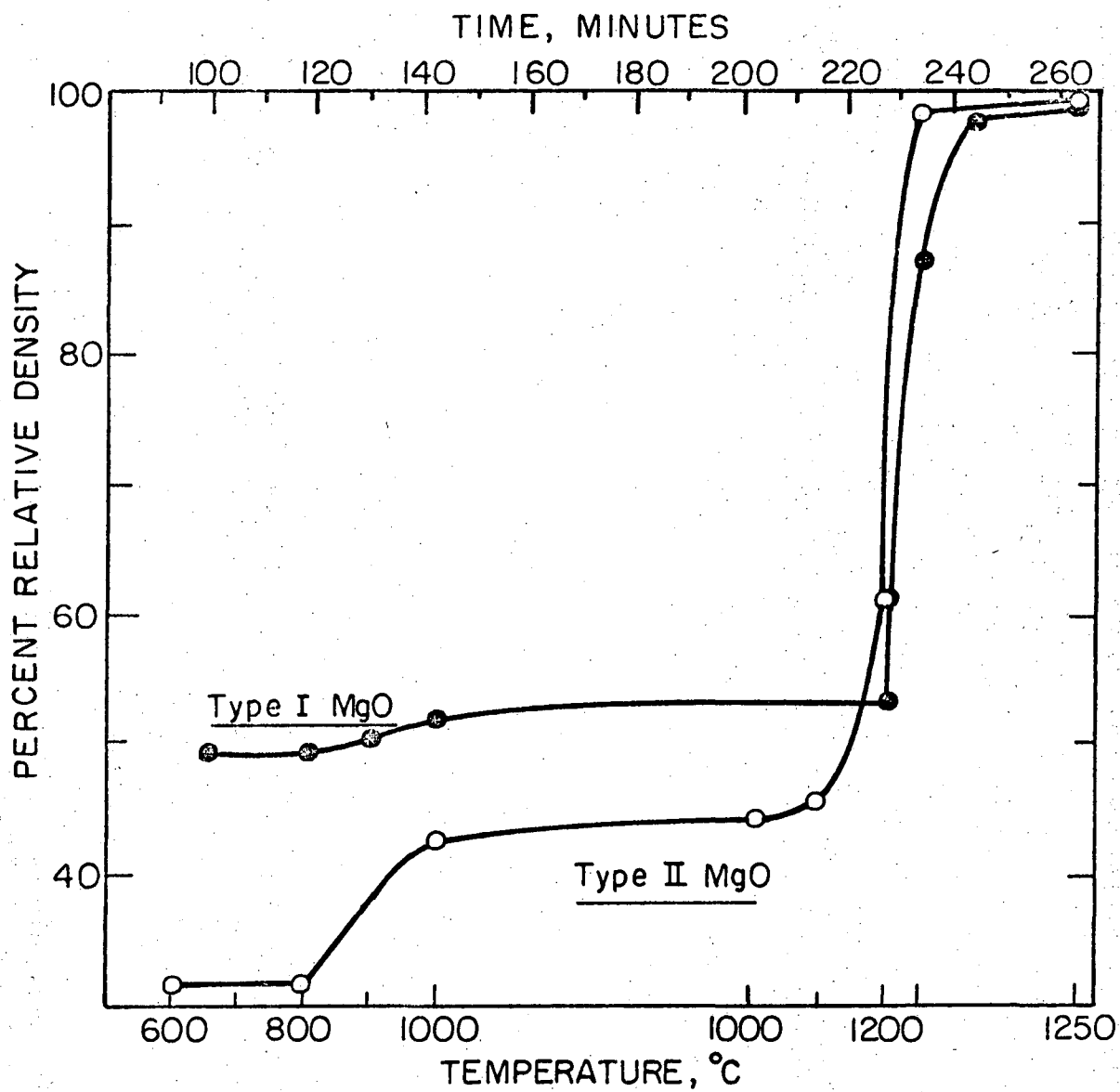
Die Used	Annealing Environment [†]	Density %	Grain Size μm	Yield Stress	Maximum Stress	Plastic Strain*
<u>Type I</u>						
Graphite		98.5	<3			
	Air	98.3	28	24,000	37,200	23.4
	Air, 24 h		60	16,000	31,600	8.8
	Vacuum	98.1	28	24,600	36,400	14.0
	Die	98.3	30	22,800	32,300	8.6
Alumina (1)		93.0	<3			
	Air	96.0	41			
	Vacuum	96.2	38			
Alumina (2)		99.0	<5			
	Air	98.6	44	20,000	34,900	10.6
<u>Type II</u>						
Graphite		99.1	<3			
	Air	98.0	84	5,300	9,050	2.4
	Air, 0 h		74	6,500	9,100	2.3
	Vacuum	98.0	90	6,000	9,900	2.4
	Die	98.5	101	6,000	10,050	2.9
Alumina		99.0	<5			
	Air	98.0	87	4,540	6,850	2.1
	Vacuum	98.3	80			

[†] All annealing times 2 h except as noted.

* At maximum stress.

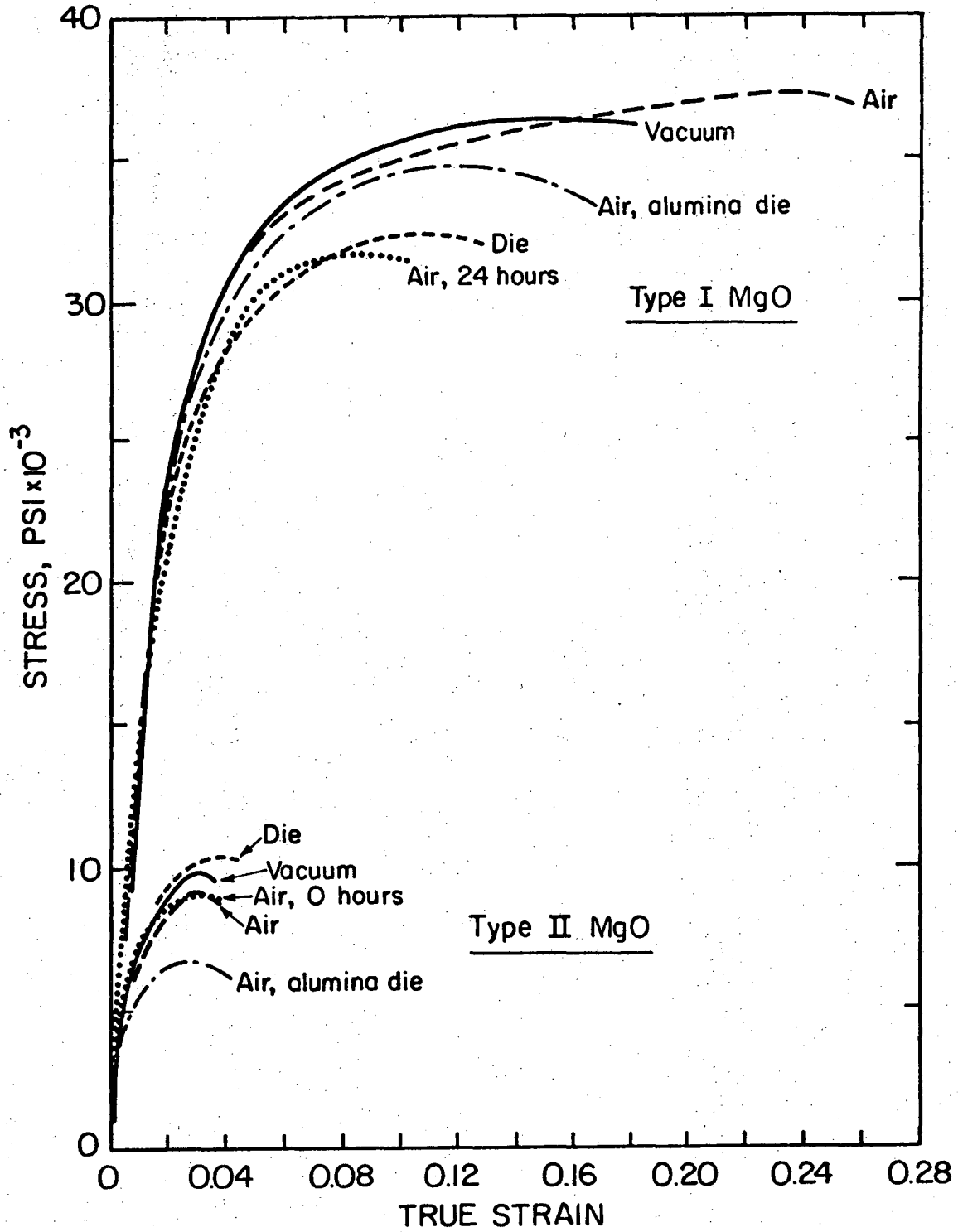
FIGURE CAPTIONS

- Fig. 1. Typical curves of density versus temperature and time during hot pressing in a graphite die.
- Fig. 2. Stress-strain curves in compression at a constant strain rate of 0.025/min. at 1200°C for specimens annealed in air, vacuum, and vacuum within a graphite die after hot pressing in graphite and alumina dies.
- Fig. 3. Schematic diagram of cracking seen after stress-strain testing in Types I and II MgO.
- Fig. 4. Fracture surface after deformation of Type I MgO hot pressed in graphite die and annealed in air.
- Fig. 5. Fracture surface after deformation of Type I MgO hot pressed in graphite die and annealed in vacuum within the graphite die.
- Fig. 6. Fracture surface after deformation of Type II MgO hot pressed in graphite die and annealed in air.
- Fig. 7. Fracture surface after deformation of Type II MgO hot pressed in graphite die and annealed in vacuum within the graphite die.



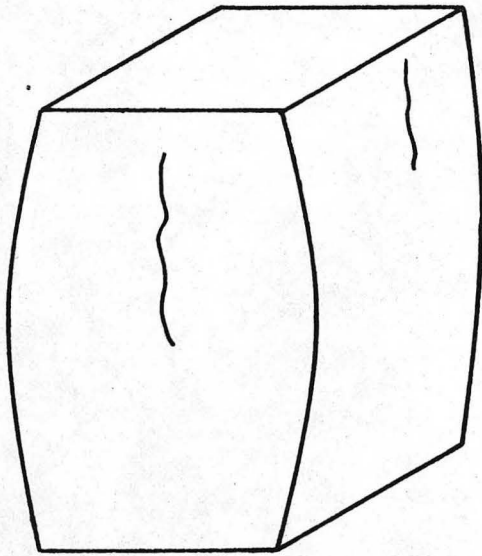
XBL 747-6843

Fig. 1.

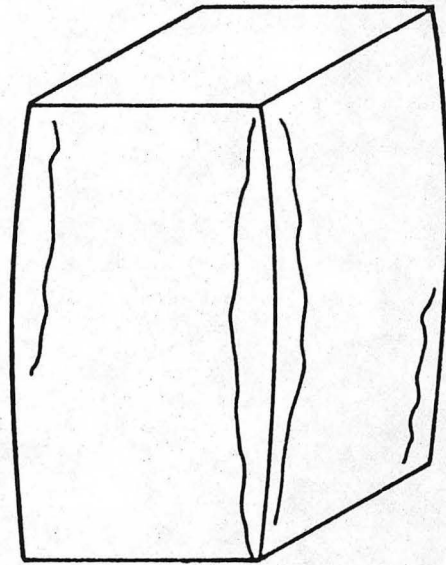


XBL 749-7120

Fig. 2.



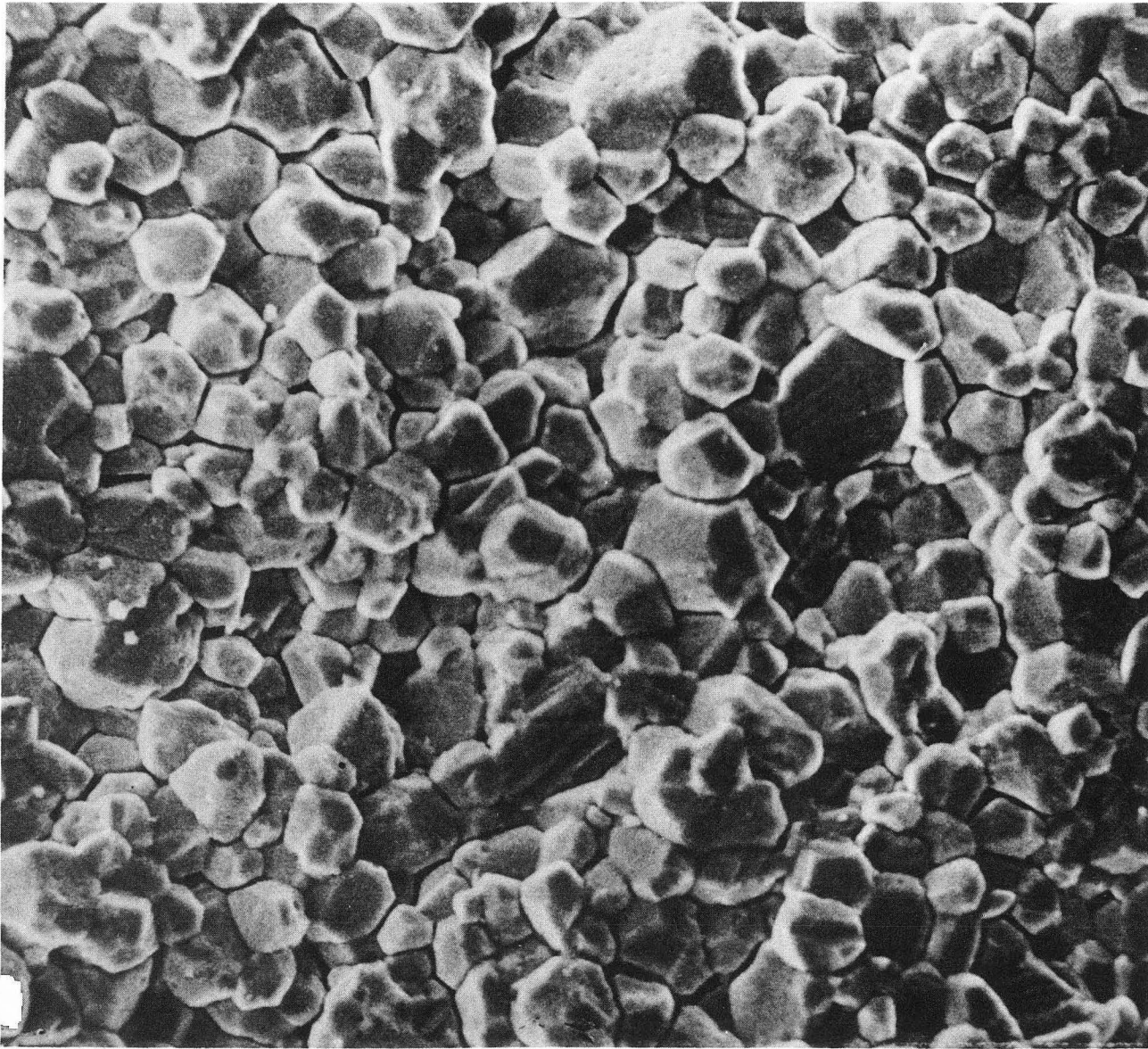
Type I MgO



Type II MgO

XBL 747-6845

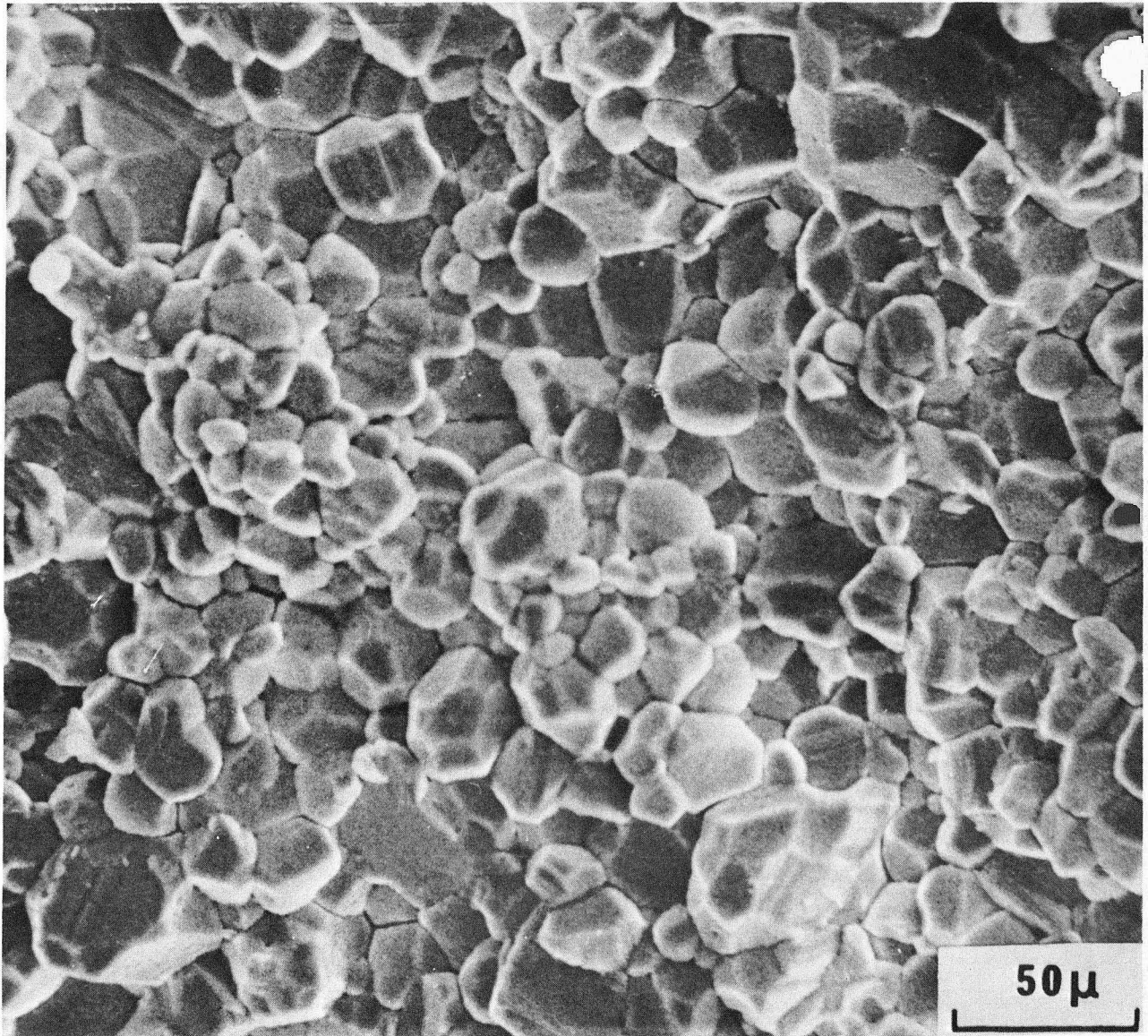
Fig. 3.



XBB 747-5192

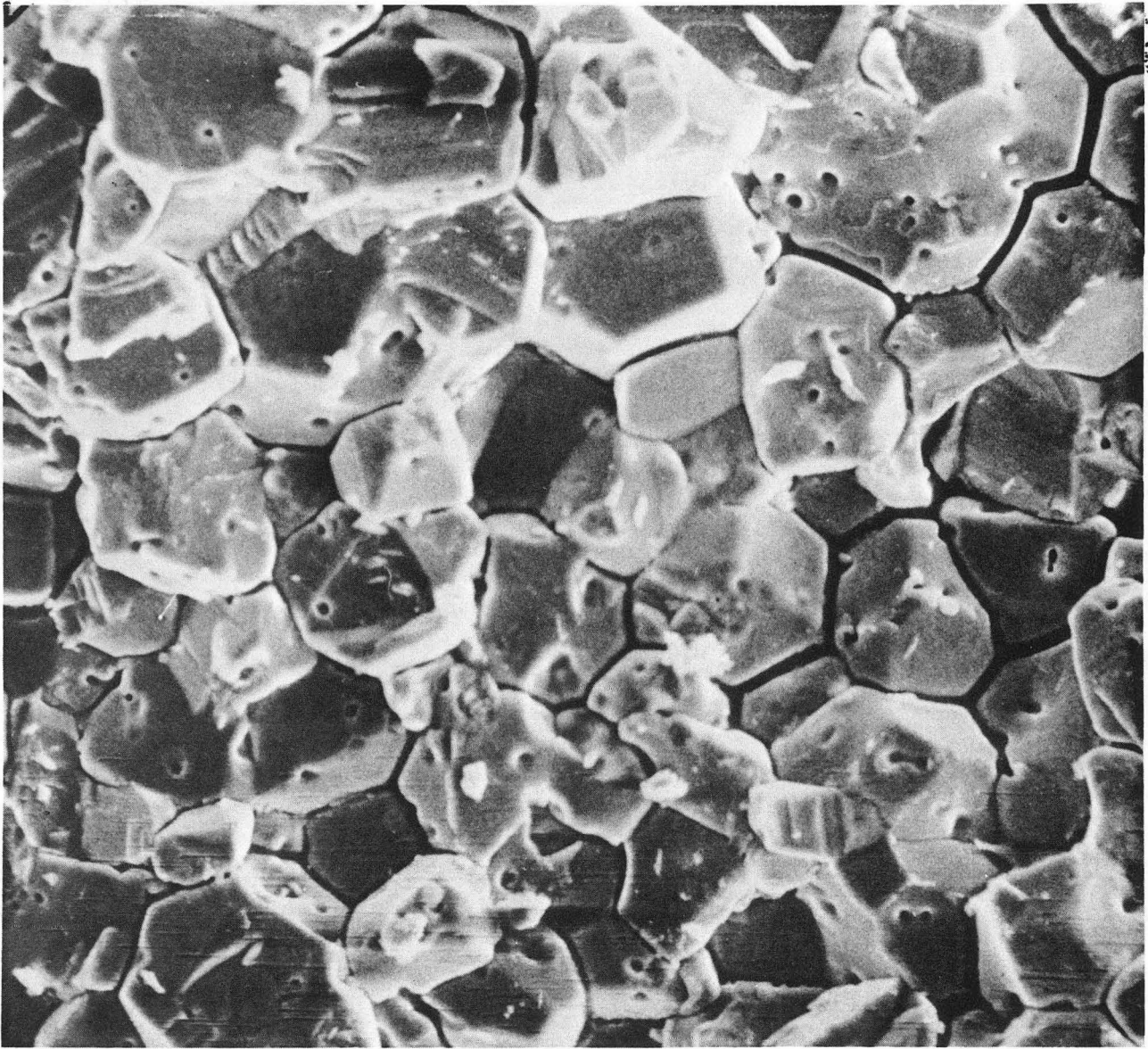
(upper)

Fig. 4.



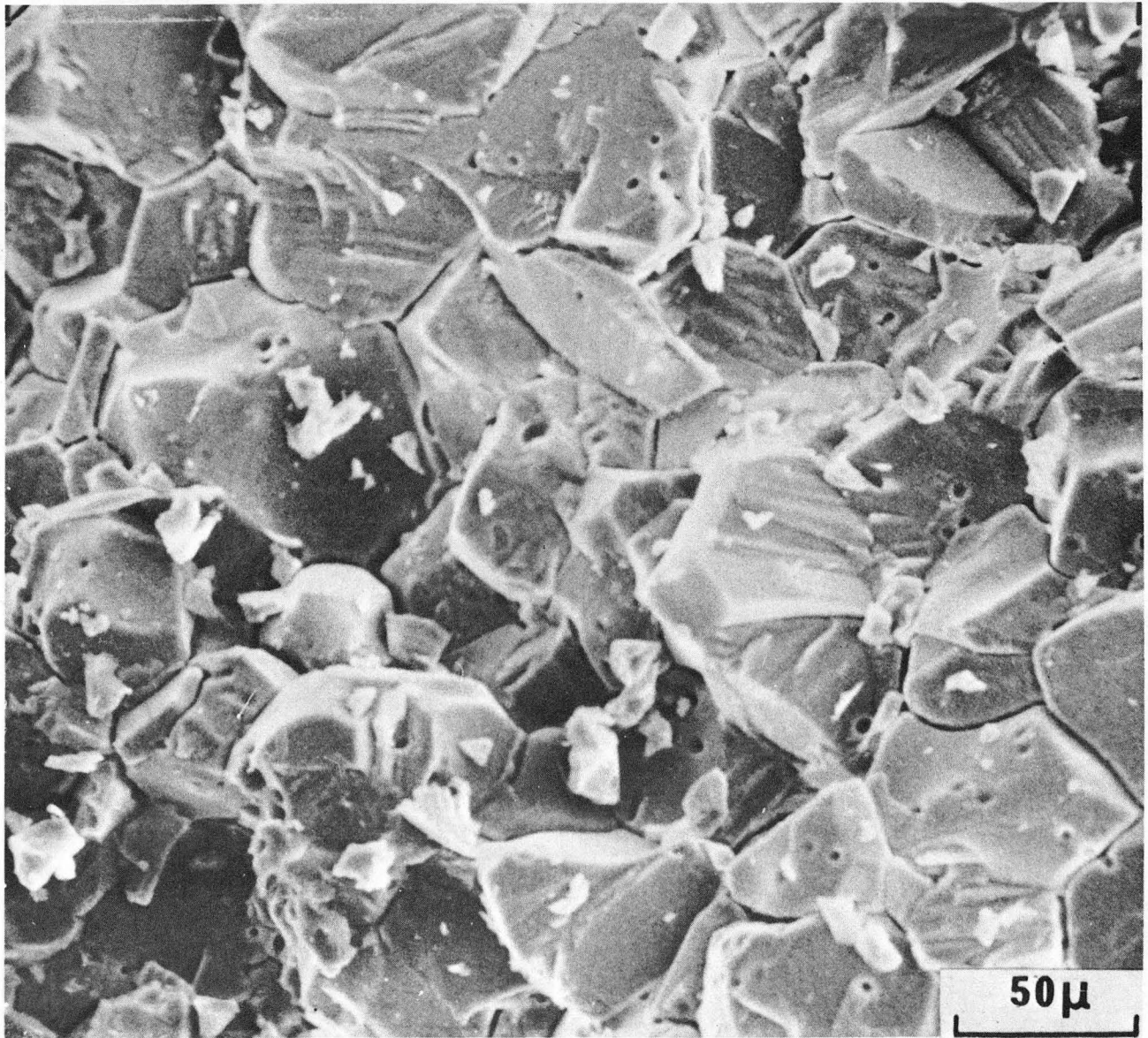
XBB 747-5192
(lower)

Fig. 5.



XBB 747-5190
(upper)

Fig. 6.



XBB 747-5190

(lower)

Fig. 7.

LEGAL NOTICE

This report was prepared as an account of work sponsored by the United States Government. Neither the United States nor the United States Atomic Energy Commission, nor any of their employees, nor any of their contractors, subcontractors, or their employees, makes any warranty, express or implied, or assumes any legal liability or responsibility for the accuracy, completeness or usefulness of any information, apparatus, product or process disclosed, or represents that its use would not infringe privately owned rights.

TECHNICAL INFORMATION DIVISION
LAWRENCE BERKELEY LABORATORY
UNIVERSITY OF CALIFORNIA
BERKELEY, CALIFORNIA 94720